Annals of Hepatology 29 (2024) 101183

Contents lists available at ScienceDirect

Annals of Hepatology

journal homepage: www.elsevier.es/annalsofhepatology

Original article

MiR-326 sponges TET2 triggering imbalance of Th17/Treg differentiation to exacerbate pyroptosis of hepatocytes in concanavalin A-induced autoimmune hepatitis

Genglin Zhang[a,#], Sensen Wu[b,#], Guangtao Xia[c,*]

[a] Biomedical Sciences College & Shandong Medicinal Biotechnology Centre, Shandong First Medical University & Shandong Academy of Medical Sciences; Key Lab for Biotech-Drugs of National Health Commission; Key Lab for Rare & Uncommon Diseases of Shandong Province, Jinan city, Shandong province 250062, PR China
[b] Department of General Surgery, Qilu Hospital of Shandong University, Jinan city, Shandong province 250012, PR China
[c] Department of Rheumatology and Immunology, Shandong Provincial Hospital Affiliated to Shandong First Medical University (Shandong Provincial Hospital), No. 324, Jingwuweiqi Road, Jinan city, Shandong province 250021, PR China

ARTICLE INFO

Article History:
Received 6 July 2023
Accepted 4 November 2023
Available online 1 December 2023

Keywords:
Autoimmune hepatitis
miR-326
Ten-eleven translocation 2
Th17/Treg
Pyroptosis

ABSTRACT

Introduction and Objectives: MicroRNA-326 is abnormally expressed in autoimmune diseases, but its roles in autoimmune hepatitis (AIH) are unknown. In this study, we aimed to investigate the effect of miR-326 on AIH and the underlying mechanism.
Materials and Methods: Concanavalin A was administrated to induce AIH in mice and the expression levels of miR-326 and TET2 was evaluated by qRT-PCR and western blot, respectively. The percentages of Th17 and Treg cells were evaluated by flow cytometry and their marker proteins were determined by western blot and ELISA. The mitochondrial membrane potential (MMP) and ROS level were tested with the JC-1 kit and DCFH-DA assay. The binding relationships between miR-326 and TET2 were verified by dual-luciferase reporter assay. The liver tissues were stained by the HE staining. In vitro, AML12 cells were cocultured with mouse CD4+T cells. The expression levels of pyroptosis-related proteins were assessed by western blot.
Results: Concanavalin A triggered AIH and enhanced the expression level of miR-326 in mice. It increased both Th17/Treg ratio and the levels of their marker proteins. The expression of TET2 was decreased in AIH mice. Knockdown of miR-326 could decrease the levels of pyroptosis-related proteins, the ROS level and increase MMP. In mouse CD4+T cells, miR-326 sponged TET2 to release IL-17A. Coculture of AML12 cells with isolated CD4+T cells from miR-326 knockdown AIH mice could relieve pyroptosis.
Conclusions: Knockdown of miR-326 exerted anti-pyroptosis effects via suppressing TET2 and downstream NF-κB signaling to dampen AIH. We highlighted a therapeutic target in AIH.

1. Introduction

Autoimmune hepatitis (AIH) is a chronic inflammatory disease regulated by autoimmune reactions. Its clinical features are elevated serum transaminases, hypergammaglobulinemia, positive autoantibodies, and histological features [1]. It mainly interfaces hepatitis with lymphocyte and plasma cell infiltration, and severe cases can rapidly progress to liver cirrhosis and liver failure [2]. Due to insidious onset of AIH and lack of effective treatment, a considerable number of AIH patients eventually develop liver cirrhosis, hepatic encephalopathy and even die [3]. Currently, glucocorticoids and immunosuppressants are commonly used. The treatment effect is often unsatisfactory with side effects such as femoral head necrosis, diabetes, infection, etc., there are many limitations and deficiencies, resulting in a decline in the quality of life of patients [4]. It is imperative to explore the pathogenesis and treatment of AIH.

MicroRNAs (miRs) are small non-coding RNAs that recognize specific target mRNAs to regulate their translation and their protein synthesis [5]. MiRNAs mediate immune system development and function and show different influences on innate and adaptive immunity [6]. Our previous study found that miR-155 was abnormally expressed in the liver tissues of AIH mice [7]. Besides, miR-326 is highly expressed in mice CD4+T cells [8] and is involved in different autoimmune diseases that used as a therapeutic target, such as

Abbreviations: AIH, autoimmune hepatitis; miR, microRNA; ALT, alanine aminotransferase; ALP, alkaline phosphatase; AST, aspartate aminotransferase; miRs, MicroRNAs; MMP, mitochondrial membrane potential; MT, mutant; PBMCs, Peripheral blood mononuclear cells; TET2, ten-eleven translocation 2; Th, T helper cell; WT, wildtype; 5hmC, 5-hydroxymethylcytosine; 5mC, 5-methylcytosine

* Corresponding author.
E-mail address: XGTxgt0412@163.com (G. Xia).
# Genglin Zhang and Sensen Wu contributed equally to this research.

https://doi.org/10.1016/j.aohep.2023.101183

autoimmune thyroiditis [9] and lupus erythematosus [10]. However, the expression level of miR-326 in AIH and its roles have not been studied.

Ten-eleven translocation 2 (TET2) protein is a DNA demethylase that belongs to the TET protein family. Specifically, TET2 converts 5-methylcytosine (5mC) to 5-hydroxymethylcytosine (5hmC) to control DNA demethylation [11]. Studies have shown that deletion of TET2 suppresses cytokine production from Th1 and Th17 cells, leading to reduced binding of 5hmC to key transcription factors [12]. TET2 is highly expressed in the hematopoietic system, and the mutation or silencing of TET2 is closely related to hematopoietic cancers [13]. Recently, Lu *et al.* have raised that TET-mediated conversion of 5mC to 5hmC contributed to the differentiation of mice CD4+ T cells. Hypermethylation occurs at high levels in the DNA of naive T cells and increased 5hmC predicts DNA demethylation and gene activation in differentiated T cells. Thus, TET regulates the transformation of naive T cells into T helper (Th)1, Th2, regulatory Treg cells and Th17 cells [14]. They have also reported that the patients with allergic rhinitis downregulated TET2 in their CD4+T cells compared with healthy donors [14]. Another literature shows that TET2 is highly expressed in normal rats' hepatocytes [15]. TET2 in B cells regulates autoimmunity by suppressing CD86 expression [16]. A recent review elucidated the inhibitory role of TET2 in autoimmunity in details [17], but the roles of TET2 in AIH remained unclear.

Evidence has shown that mitochondrial oxidative stress and the NLRP3 inflammasome plays an important role in pyroptosis in human hepatocytes [18]. NLRP3 is an intracytoplasmic immunosensor protein related to pyroptosis. The main features of pyroptosis are the cleavage of caspase-1 and GSDMD-N-terminal, and the secretion of inflammatory factors such as IL-1β. As an innate immune barrier, pyroptosis can resist the invasion of external pathogens. But it can induce various long-term chronic inflammatory diseases. In AIH, NF-κB pathway and the assembly of the NLRP3 inflammasome are activated [19], and NLRP3 induces further inflammation and pyroptosis [20]. In addition, it has been shown in the literature that IL-17, the main secretory factor of Th17, is one of the important activators of pyroptosis, and induces normal cell pyroptosis in rheumatoid arthritis [21,22] and pneumonia-induced sepsis [23]. IL-17A can destroy mitochondrial function by binding to IL-17R on cells, thereby releasing ROS, activating NF-κB pathway, and inducing pyroptosis [24].

Concanavalin A-induced liver injury model is considered to be a CD4+ T helper cell (Th) activation model in AIH [25]. AML12 cells have been used in several autoimmune hepatitis studies [26,27]. Therefore, we established AIH mouse model using concanavalin A and AML12 cells were cocultured with CD4+T cells to investigate the effects of miR-326 and its potential target in AIH, and provide potential therapeutic options for AIH.

2. Material and methods

2.1. Mice

Male C57BL/6 mice (6-8-week old) (Changsheng, China) were housed under 12 h light/dark cycles with food and water supply. Concanavalin A was injected at a dose of 20 mg/kg via tail vein, and the level of miR-326 was measured at different time points (0, 6, 12, 24, 48, 72 h) in liver tissue. To knock down intrinsic miR-326, 100 nmol of antagomiR-326 (KD-miR-326) or negative control antagomiR-NC (KD-NC) (GenePharma, China) were injected into tail vein of mice before the establishment of the AIH model. Mice were assigned into blank group, AIH group, AIH+KD-NC group and AIH+KD-miR-326 group. After knockdown of miR-326 in mice, concanavalin A was injected via the tail vein to trigger AIH. 48 h later, the mice were anesthetized using thiopental (40 mg/kg, ip). Blood was obtained from the retro-orbital plexus. Then, mice were euthanized by carbon dioxide asphyxiation and liver tissues were rapidly isolated for subsequent experiments [7,28,29].

2.2. Cell culture, coculture and transfection

Peripheral blood mononuclear cells (PBMCs) were isolated using Lymphocytes separation medium (Dakewe, China). PBS was added to the blood and transferred into 5 ml separation medium. After centrifuging at 500 g for 0.5 h, PBMCs were collected.

CD4+ T cells were isolated from the liver using the Mouse CD4+ T cell isolation kit (nwbiotec, China). After verifying the purity, 1×10^4 cells/mL of CD4+ T cells were inoculated in 5 mL X-Vivo 15 medium (Lonza, Switzerland) with 10 % autologous serum and 100 U/mL antibiotics.

Murine AML12 cells were inoculated in DMEM/F-12 (Procell, China) containing ITS supplement (Procell, China) and FBS (Procell, China). A total of 1×10^5 AML12 cells were cultured for 24 h and then cocultured with mouse 1×10^6 CD4+ T cells for 48 h, and then collected for subsequent experiment [30].

To knock down and over express miR-326, CD4+T cells were transfected by miR-326 inhibitor (KD-miR-326) / negative control (KD-NC) and miR-326 mimic / mimic NC, respectively. siRNA TET2 was transfected into CD4+T cells to knock down TET2. The transfection was performed by Lipofectamine 3000 (Invitrogen, USA).

2. 3 qRT-PCR

RNA extraction was conducted with RNApure Kit (Bioteke, China). The reverse transcription was performed with Super M-MLV Kit (Yeasen, China). QRT-PCR was executed with the QuantStudio 7 Pro System (ABI, USA) using the SYBR Green Realtime PCR Master Mix (Solarbio, China) and 2 × Power Taq PCR Master Mix (Bioteke, China). Primer sequences were shown in Table 1. U6 was used as the internal control gene of miR-326 and β-actin was used as the internal control gene of TET2. Relative expression levels were normalized by the $2^{-\Delta\Delta Ct}$ method.

2.4. Western blot

Proteins were extracted with RIPA Lysis Buffer (Solarbio, China) and quantified using a BCA Kit (Solarbio, China). After separation via SDS-PAGE (Genscript, China) and transferring to the PVDF membrane (Merck, USA), primary antibodies against TET2 (1:1000, Abcam, USA), FOXP3 (1:1000, Abcam, USA), RORγT (1:1000, Abcam, USA), NLRP3 (1:1000, Abcam, USA), IL-1β (1:1000, Abcam, USA), cleaved caspase 1 (1:1000, CST, USA), GSDMD-N (1:1000, Abcam, USA), TNF-α (1:1000, Abcam, USA), p-IκBα (1:1000, Abcam, USA), IκBα (1:1000, USA), p-P65 (1:1000, Abcam, USA), IκBα (1:1000, Abcam, USA), GAPDH (1:5000) and β-actin (1:5000) (Abcam, USA) were administrated at 4°C for 12 h. Next, secondary HRP-conjugated antibody (1:2000) was added and incubated for 1 h. The bands were visualized with a DAB kit (Solarbio, China). The relative expression levels were calculated via Image J 1.53H (NIH, USA).

Table 1
The primer sequences for RT-qPCR.

Primer	sequences
miR-326	(forward) 5'-CTTGTTACGGTACTCGG-3' (reverse) 5'-CACTCTATGTGGCAGCTTA-3'
U6	(forward) 5′-CACGGATCCTGCAACTAA-3′ (reverse) 5′-TGCGCAGTTAGAGTCAGG-3′
TET2	(forward) 5′-GTGCCTGAACGATACCAGAA-3′ (reverse) 5′-CAGAAGCAACTCTCGGTAGG-3′
β-actin	(forward) 5'-CACGAAACTACGTGCAGCTCC-3' (reverse) 5'- CATACTCATGCATGCTGATC-3'

2.5. ELISA

The levels of IL-10, IL-17A and IL-23 were determined by ELISA kits (MultiScience, China) and the indicators of liver function (ALT, AST and ALP) were assessed by detection kits (Jiancheng, China).

2.6. Hematoxylin-eosin (HE) staining

Mouse liver tissues were stored in 10 % formalin (Solarbio, China). For HE staining, the samples were resected, fixed in 4 % paraformaldehyde (Hushi, China) and embedded. The slides were sectioned and stained with H&E staining kit (Solarbio, China), and observed under the microscope (Olympus, Japan).

2.7. Dual-luciferase reporter assay

The binding relationship was detected by Promega Luciferase Assay System (Promega, USA). Wildtype (WT) TET2 containing miR-326 binding site and mutant (MT) TET2 without miR-326 binding site were sub-cloned into PsiCHECK2 luciferase reporter vectors. Then, the vectors and miR-326 mimic / mimic-NC were co-transfected into CD4+T cells. Forty-eight hour later, relative luciferase activity (Luciferase/Renilla) was determined.

2.8. Flow cytometry

To obtain a single-cell suspension, mouse liver tissues were homogenized and washed by PBS. Collagenase was added for digestion at 37°C for 4 h. Disperse cells and tissue fragments were separated through 70-μm nylon cell strainers. Cell suspensions were washed twice by PBS. Re-suspension of the precipitation with 33 % Percoll superimposed on 70 % Percoll solution in another centrifuge tube. After spinning at 2400 rpm for 25 min, the white blood cell layer at the interface of 2 layers of Percoll solution was absorbed into another centrifuge tube and was spun at 800 rpm for 5 min following washing with 1 $\times$ PBS solution for twice. The collected cells were lymphocytes [31].

To evaluate the percentage of T cells in liver lymphocytes, cells were stained with FITC anti-CD3 antibody (ab239226, Abcam) plus Alexa Fluor 488 anti-CD4 antibody (ab252149, Abcam). To determine the proportion of Treg cells and Th17 cells, Alexa Fluor 488 anti-CD4 antibody (ab252149, Abcam) plus APC anti-FOXP3 (ab200568, Abcam) or Alexa Fluor 488 anti-CD4 antibody (ab252149, Abcam) plus APC anti-IL-17A (17-7177-81, Thermo Fisher, USA) were applied respectively. The samples were analyzed using CytoFLEX (Beckman-Coulter, USA).

The apoptosis of AML12 cells was assessed using an Annexin V-FITC/PI staining kit (Beyotime, China). The cells were treated with Annexin V-FITC and PI accordingly and analyzed using the CytoFLEX (Beckman-Coulter, USA).

2.9. ROS assay

ROS level was checked using the DCFHDA kit (Abcam, USA). The supernatant was obtained from fresh liver tissue homogenized and administrated by 10 μM DCFDA diluent for 30 min. AML12 cells were incubated in 6 well plates (10^6 cells/well) and cultured for 24 h. DCFDA 10 μM diluent was administrated for 30 min and cells were washed by serum-free medium for three times. Fluorescence was recorded by a Varioskan LUX multiplate reader (Thermo Fisher, USA) with a wavelength of 485 nm/535 nm.

2.10. Evaluation of mitochondrial membrane potential (MMP)

The JC-1 MMP Assay Kit (Abcam, USA) was selected to detect MMP. Minute^{TM} Mitochondria Isolation kit (Invent Biotechnologies, USA) was used to extract mitochondria in liver tissue according to the manufacturer's instruction [32]. Briefly, 0.9 ml JC-1 solution was mixed with 0.1 ml of 100 μg extracted mitochondria. And AML12 cells were collected and stained with JC-1 solution. Higher MMP would trigger aggregation of JC-1 to show red fluorescence while JC-1 would stay as monomers and show green fluorescence due to low MMP. Excitation wavelength 485 nm, emission wavelength 590 mm. The results were captured by a fluorescence spectrophotometer.

2.11. MTT assay

AML12 cells (10^4 cells/well) were maintained in 96-well plates. Then, 10 μL 5 mg/ml MTT (Solarbio, China) was added and maintained for 4 h. Then the formazan crystals (Solarbio, China) were dissolved with 150 μL dimethyl sulfoxide (DMSO; Solarbio, China). OD value was measured at 490 nm by a Varioskan LUX multiplate reader (Thermo Fisher, USA).

2.12. Statistical analysis

The experiments were performed in triplicate and repeated for three times. Data were expressed as mean $\pm$ SEM. Graphpad Prism 9.3.1 was used for data analyses. The differences were analyzed by Student's t-test or one-way ANOVA. $P<0.05$ indicated a statistical significance.

2.13. Ethical statement

All animal experiments complied with the Animal Research: National Institutes of Health guide for the care and use of Laboratory animals (NIH Publications No. 8023, revised 1978). This research was approved by the Animal Care Committee of Shandong Provincial Hospital Affiliated to Shandong First Medical University and followed the Guide for the Care and Use of Laboratory Animals.

3. Results

3.1. Knockdown of miR-326 ameliorated the immune imbalance in mice AIH model

qRT-PCR was to evaluate the expression level of miR-326 in the liver tissue of concanavalin A-induced AIH mice, and the result showed that the expression of miR-326 was increased in a time-dependent manner before 48 h and significantly elevated at 48 h and 72 h, and miR-326 expression was highest at 48 h. It may be due to massive necrosis of hepatocytes that the expression of miR-326 at 72 hours is lower than that at 48 hours. Based on this, 48 h was chosen as the appropriate time point for concanavalin A treatment (Fig 1A). After that, the expression of miR-326 in mice after administration of KD-miR-326 or KD-miR-NC for 48 h was verified, and miR-326 expression was successfully inhibited in KD-miR-326 group (Fig 1B). AIH group had a higher expression level of miR-326 in contrast to blank group and miR-326 expression was lower in AIH+KD-miR-326 group compared with AIH+KD-NC group (Fig 1C). Moreover, AIH group had a higher level of liver function indicators (ALT, AST and ALP) compared with blank group, this indicated hepatotoxicity in AIH mice. Knockdown of miR-326 decreased the levels of liver function indicators in AIH+KD-miR-326 group, this proved that knockdown of miR-326 ameliorated concanavalin A-induced liver damage in mice (Fig 1D). Next, it was reported that the percentage of CD3+/CD4+ cells in the AIH group was increased and AIH+KD-miR-326 group had a lower level of CD3+/CD4+ cells compared with AIH +KD-NC group (Fig 1E). In addition to this, the effects of miR-326 inhibition on the differentiation of Treg cells and Th17 cells were explored by flow cytometry. Both the percentages of Treg cells (Foxp3+/CD4+) and Th17 (IL-17A+/CD4+) cells in AIH group were

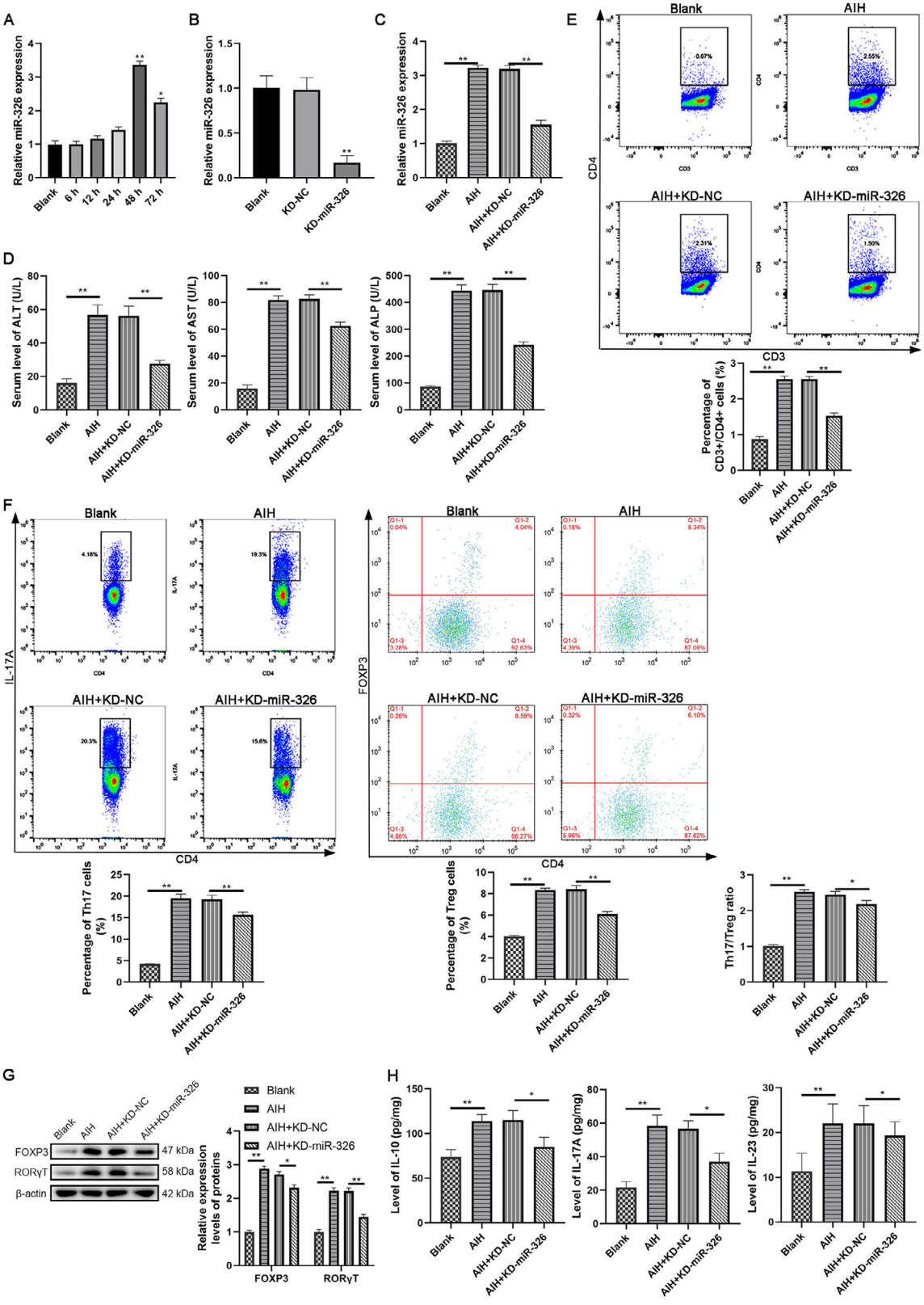

Fig. 1. Knockdown of miR-326 ameliorated AIH in mice. (A) The expression level of miR-326 was detected by qRT-PCR in concanavalin A-induced AIH mice at different time points. (B) The expression level of miR-326 was detected by qRT-PCR in mice treated with antagomiR-326 or antagomiR-NC. (C) The expression level of miR-326 was detected by qRT-PCR in AIH mice treated with antagomiR-326 or antagomiR-NC. (D) The liver function of mice was tested by commercial kits. (E) The percentage of CD3+/CD4+T cells in mice was evaluated by flow cytometry. (F) The percentage of Th17 and Treg cells in liver tissue was evaluated by flow cytometry. (G) The expression of protein markers of Th17 and Treg cells in liver tissue were detected by western blot. (H) The levels of protein markers of Th17 and Treg cells in mice were evaluated by ELISA. *: $P < 0.05$ and **: $P < 0.01$. ALT, alanine aminotransferase; AST, aspartate aminotransferase; ALP; alkaline phosphatase.

higher in contrast to blank group, and the Th17/Treg ratio was also increased, whereas the percentages of both Treg and Th17 cells and the Th17/Treg ratio were lower after the treatment of KD-miR-326. (Fig 1F). Next, the results showed that the levels of Treg cell markers (FOXP3 and IL-10) and Th17 cell markers (RORγT, IL-17A and IL-23) were higher in AIH group compared with blank group. Knockdown of miR-326 in AIH+KD-miR-326 group decreased their expression levels compared with that in AIH+KD-NC group (Fig 1G-H). This indicated that knockdown of miR-326 suppressed the Treg/Th17 cells differentiation and ameliorated immune imbalance in mice.

3.2. Knockdown of miR-326 inactivated NF-κB pathway and ameliorates pyroptosis in mice AIH model

It was observed that the administration of concanavalin A triggered liver focal necrosis and inflammatory infiltration that the arrows point to in AIH and AIH+KD-NC groups compared with blank group. And these symptoms were mitigated in AIH mice treated with KD-miR-326 (Fig 2A). HE result also indicated that the morphology and arrangement of hepatocytes were normal in blank group, and inflammatory cell infiltration, degeneration vacuolization and massive necrosis occurred in liver tissue in AIH and AIH+KD-NC groups, and knockdown of miR-326 alleviated the inflammatory and necrosis in AIH+KD-miR-326 group (Fig 2B). Besides, IL-17 could induce mitochondrial damages to release ROS and activate NF-κB pathway [24]. In order to investigate the mechanism of miR-326 in concanavalin A-induced liver inflammatory response, ROS level and MMP were evaluated. It was reported that AIH group had a higher level of ROS and a lower level of MMP compared with blank group. Knockdown of miR-326 exerted anti-oxidative and protective effects via reducing ROS level and enhancing MMP in AIH+KD-miR-326 group (Fig 2C-D). Moreover, Western blot result showed that concanavalin A treatment upregulated the expression levels of pyroptosis-related proteins and activated NF-κB signaling pathway, whereas knockdown of miR-326 ameliorated pyroptosis and inactivated NF-κB signaling pathway (Fig 2E). These results revealed that knockdown of miR-326 inactivated NF-κB pathway and dampened the pyroptosis of hepatocytes in concanavalin A-induced AIH mice.

3.3. MiR-326 sponged TET2 in mice CD4+T cells, promoted the production of IL-17A and induced differentiation of Th17 cells

qRT-PCR and western blot results reported that AIH group had a lower expression level of TET2 in contrast to blank group in the liver tissues of AIH mice. The expression of TET2 was higher in AIH+KD-miR-326 group in contrast to AIH+KD-NC group in the liver tissues of AIH mice (Fig 3A-B). To detect the relationship of miR-326 and TET2 in AIH, Pearson's correlation test was used to analyze the expression of miR-326 and TET2 in liver tissues of AIH mice. R^2 was 0.4629, and indicated that the expression level of miR-326 was negatively correlated with TET2 mRNA (P=0.0437, Fig 3C). Using ENCORI, we found that miR-326 could bind to TET2 mRNA complementarily, this predicted that there was a targeting relationship between them (Fig 3D). This was verified by dual-luciferase reporter assay. miR-326 decreased the relative luciferase activity in miR-326 mimic+TET2 WT group, and there was no significant difference among relative luciferase activity of other groups (Fig 3E).

Then the transfection efficiency of knockdown and overexpression miR-326 in isolated CD4+T cells in mice was verified by qRT-PCR (Fig 3F). After that, it was found that overexpression of miR-326 inhibited the expression of TET2, whereas knockdown of miR-326 exerted opposite effects in transfected CD4+T cells (Fig 3G-H). After verifying the transfection efficiency of si-TET2 using qRT-PCR and western blot (Fig 3I-J), ELISA result verified that knockdown of miR-326 reduced the secretion of IL-17A, which could subsequently suppress the differentiation of Th17 cells. And this impact was reversed

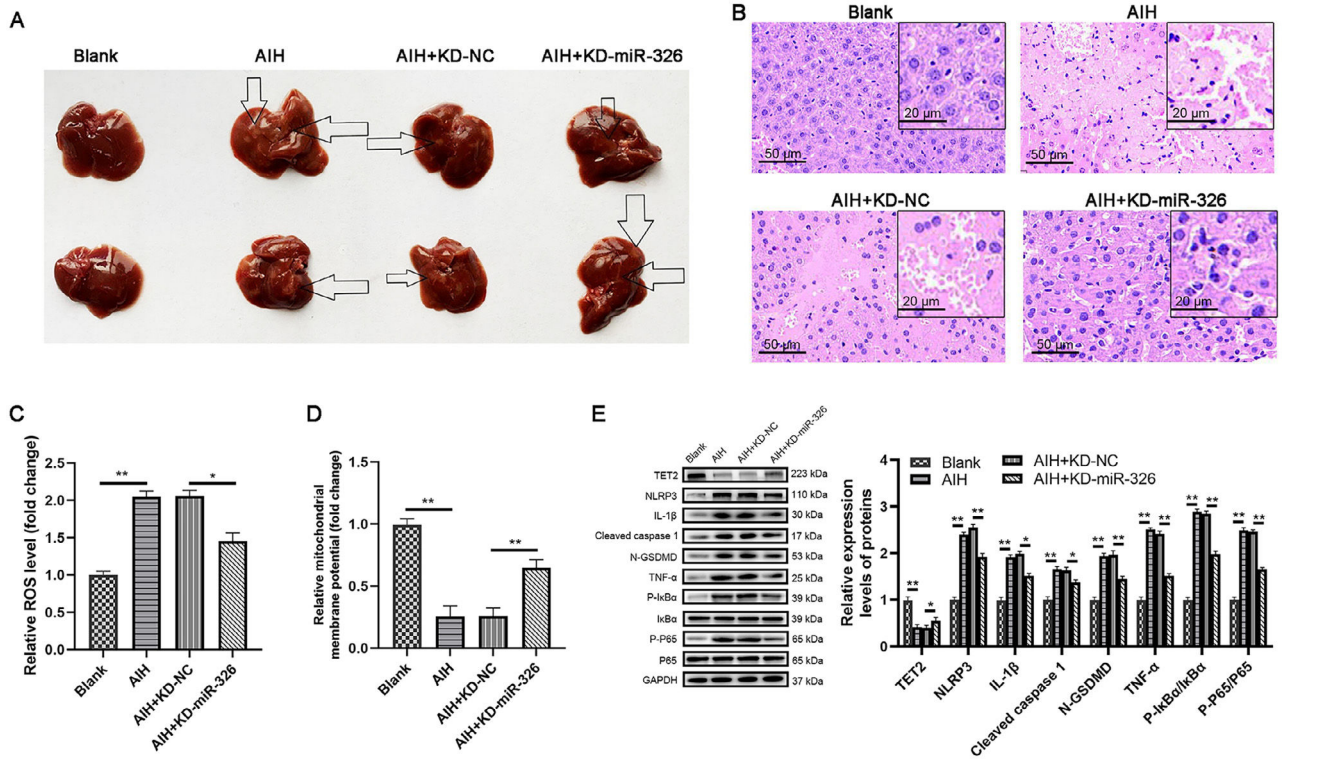

Fig. 2. Knockdown of miR-326 protected mitochondria and ameliorated pyroptosis of hepatocytes in AIH mice. (A) The images of mouse liver. Arrowhead: focal necrosis and inflammatory infiltration. (B) HE staining of mouse liver tissues 200× magnification, scale = 50 μm; 400× magnification, scale = 20 μm). (C) ROS level was measured by DCFHDA assay. (D) MMP was measured by JC-1 assay. (E) The expression levels of pyroptosis-related proteins and NF-κB pathway-related proteins were determined with western blot. *: $P < 0.05$ and **: $P < 0.01$.

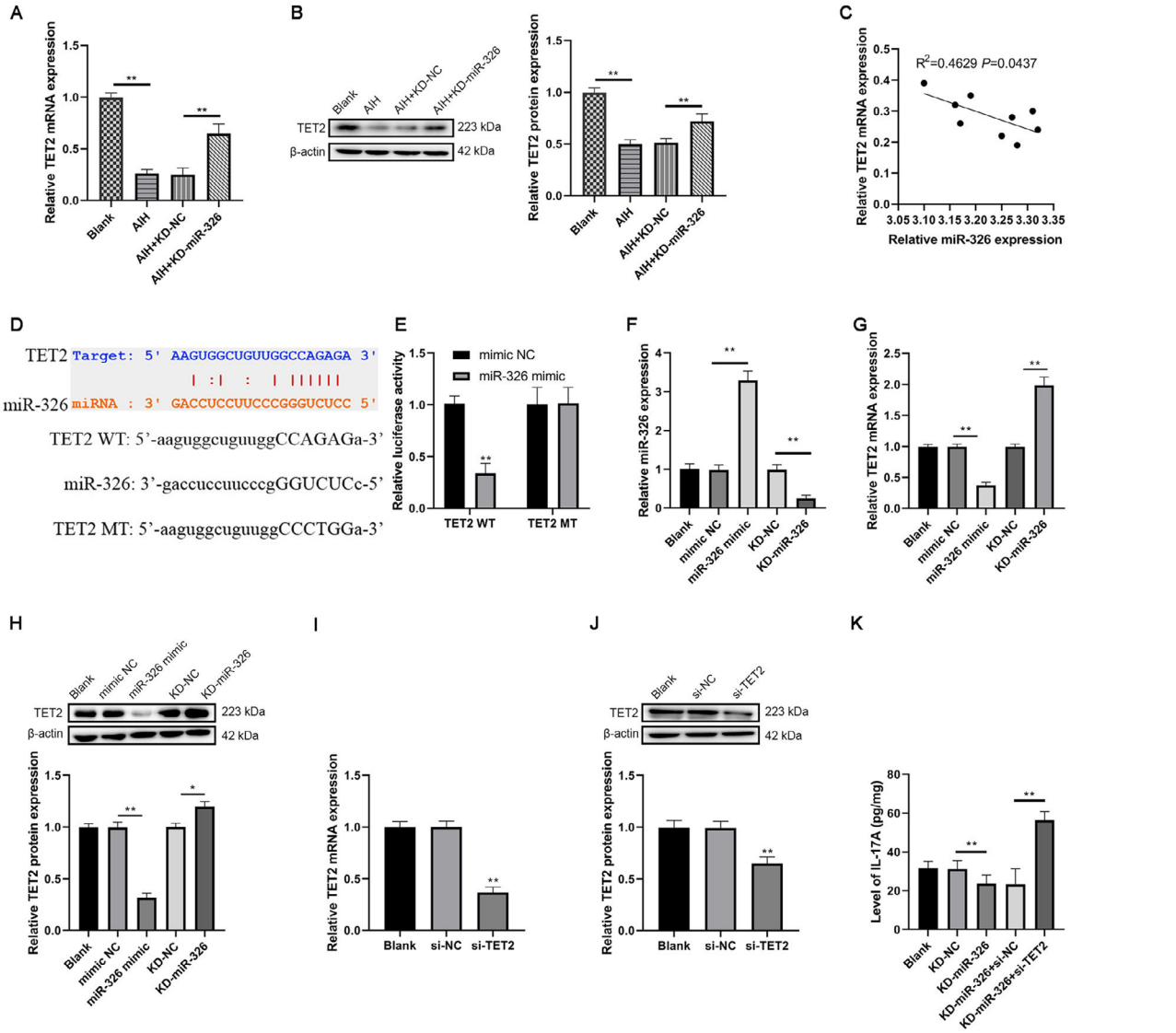

Fig. 3. miR-326 sponged TET2 in mice CD4+T cells and promoted the production of IL-17A. (A) and (B) The expression of TET2 in mice was detected by qRT-PCR and western blot, respectively. (C) The relationship between the levels of miR-326 and TET2 mRNA in liver tissue of AIH mice was analyzed by Person's correlation test. The binding relationship between miR-326 and TET2 in mice was (D) predicted by ENCORI and (E) verified by the dual-luciferase reporter assay. (F) The transfection efficiency was verified by qRT-PCR. (G) and (H) The expression level of TET2 was detected in miR-326 mimic or KD-miR-326 transfected CD4+T cells by qRT-PCR and western blot, respectively. (I) and (J) The transfection efficiency was verified by qRT-PCR and western blot, respectively. (K) The level of IL-17A was tested by ELISA. *: $P < 0.05$ and **: $P < 0.01$.

by knockdown of TET2 (Fig 3K). These results indicated that miR-326 sponged TET2 in mice CD4+T cells and increased the production of IL-17A to promote the differentiation of Th17 cells.

3.4. Knockdown of miR-326 ameliorated the pyroptosis of AML12 cells cocultured with mouse CD4+T cells

The CD4+T cells in PBMCs of four groups of mice was obtained. AML12 were cocultured with CD4+T cells for 48 h. MTT assay result showed that the viability of AML12 cells in AIH group was decreased. Knockdown of miR-326 rescued the decrease of cell viability caused by AIH in AIH+KD-miR-326 group (Fig 4A). Flow cytometry showed similar findings. Coculture of AML12 cells with CD4+T cells in AIH group upregulated the apoptotic rate of AML12 cells, whereas these effects were counteracted by knockdown of miR-326 (Fig 4B).

Then ROS level and MMP in cocultured AML12 cells were also evaluated. The cells in AIH group had a higher level of ROS and a lower level of MMP compared with blank group. Knockdown of miR-326 exerted anti-oxidative and protective effects via decreasing ROS level and enhancing MMP (Fig 4C-D). Last but not least, the results exhibited that the cocultured AML12 cells in AIH group expressed higher levels of pyroptosis-related proteins in contrast to those in blank group. Knockdown of miR-326 neutralized the cell pyroptosis by reducing the expression levels of pyroptosis-related proteins in AIH+miR-326 group. These results above revealed that the knockdown of miR-326 ameliorated the pyroptosis of AML12 cells cocultured with CD4+T cells.

4. Discussion

Currently, an increasing prevalence of AIH is observed globally, with a relative increase in the percentage of male patients [33]. It is of great significance to investigate the pathogenesis of AIH and effective drugs. Due to the development of basic immunology, the diagnosis and treatment of immune diseases have advanced rapidly. In particular, biological therapy has achieved certain results in systemic lupus erythematosus and rheumatoid arthritis. But unfortunately,

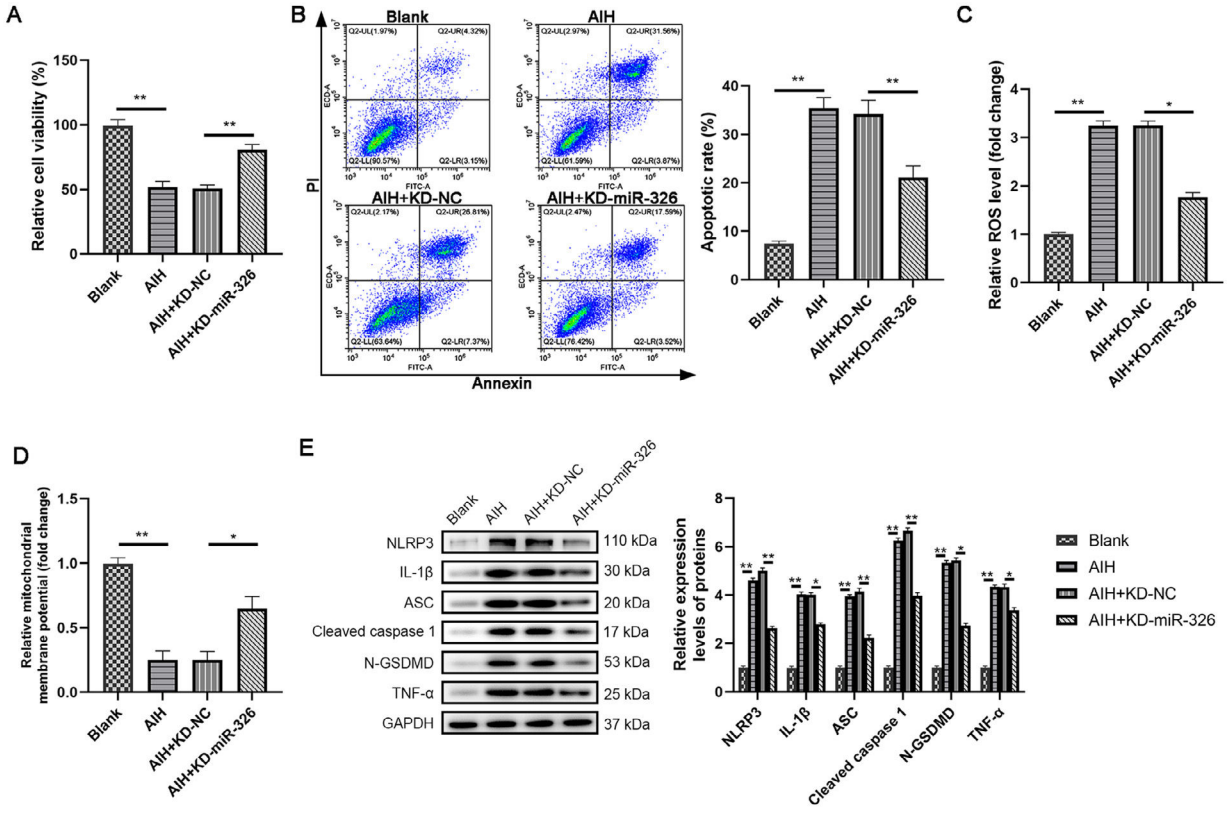

Fig. 4. Knockdown of miR-326 ameliorated the pyroptosis of cocultured AML12 cells. (A) The viability of cocultured AML12 cells was examined by MTT assay. (B) The apoptotic of cocultured AML12 cells was detected with flow cytometry. (C) ROS level was measured by the DCFHDA assay in AML12 cells. (D) The MMP was measured by JC-1 assay. (E) The expression of pyroptosis-related proteins was determined with western blot. *: $P < 0.05$, **: $P < 0.01$.

the treatment of AIH has been in the blank, which is the research motivation of this study.

Liver is an immune organ rich in immune cells. Inflammatory cytokines could accelerate the autoimmune process, and it is the main pathogenesis of concanavalin A-induced hepatitis [7]. In AIH, autoimmune-induced liver damage is triggered by CD4+T cells. CD4 +T lymphocytes are important immune cells, which can be differentiated into Th1 cells, Th2 cells, Th17 cells and Treg cells under the induction of different cytokines. Furthermore, activated T cells in AIH will break the balance between Treg and Th17 cells. This is an important hallmark of AIH, and modulating Treg/Th17 balance may be a potential therapeutic approach for AIH. Treg cells use Foxp3 and IL-10 as differentiation markers to control autoimmune suppression. Th17 cells are a newly discovered class of T lymphocyte subsets with IL-17A and IL-23 as differentiation markers, and are mediated by the transcription factor RORγt. Th17 cells mainly promote inflammation [34]. Our previous study reported abnormal accumulation of both Treg and Th17 cells and upregulated Th17/Treg ratio after administration of concanavalin A [7]. In this study, similar results were observed.

MiRNAs are involved in the control of growth, development, aging, and apoptosis of organisms. More than 100 miRNAs are expressed in immune cells and control innate and adaptive immunity. As important post-transcriptional regulators, microRNAs are abnormally expressed in different diseases. In Behcet's disease [35] and multiple sclerosis [36], miR-326 regulates the occurrence and development of autoimmune diseases by controlling its target genes, affecting the expression of various cytokines or the activity of transcription factors. In heart transplantation patients, miR-326 can be used as an indicator for early diagnosis of rejection. Patients with elevated miR-326 have a high chance of rejection [37]. In patients with multiple sclerosis, miR-326 regulates the differentiation of Th17 cells by acting on the target gene Ets1. Animal studies further confirmed that the level of miR-326 was associated with the severity of the disease [9]. Increased expression of miR-326 was found in patients with type I diabetes [38]. MiR-326 is overexpressed in patients with systemic lupus erythematosus, and miR-326 affects the differentiation and proliferation of B cells through Ets-1 to trigger the pathogenesis of systemic lupus erythematosus [39]. In people with Behcet's disease, it was found that miR-326 was highly expressed in PBMCs [40]. Another study found that miR-326 could activate NF-κB pathway to exacerbate inflammation [41].

The ENCORI database predicted that miR-326 could target TET2. In autoimmune myelodysplastic syndromes, TET2 mutation and deletion are closely associated with the progress of the disease and inflammatory response [13]. In type 1 diabetes, TET2 has been shown to regulate immune cell function and immune response, and loss of TET2 allows beta cells to be attacked and destroyed by autoimmune cells [42,43]. Some miRNAs, such as miR-22, miR-26a, miR-29 and miR-125b, have been shown to target the expression of TET2. Targeted inhibition of TET2 expression can promote cellular inflammatory pyroptosis [44]. TET2 has a role in the regulation of inflammation [45]. There is also evidence that TET2 can inhibit the activation of NF-κB P65, and that miR-210 can target and inhibit the expression of TET2, which can activate NF-κB pathway [46]. Last but not least, IL-17A can destroy mitochondrial function by binding to IL-17R on cells, thereby releasing ROS, activating NF-κB pathway, and inducing pyroptosis [24].

5. Conclusions

The expression of miR-326 was upregulated in AIH mice. Knockdown of miR-326 exerted beneficial effects by ameliorating pyroptosis of hepatocytes via sponging TET2 and inactivation of NF-κB

pathway. This study might provide a potential molecular therapeutic target or diagnostic biomarkers for AIH.

Declaration of interests

None.

Author contributions

Genglin Zhang: Investigation, Methodology, Resources, Supervision, Visualization, Writing – original draft. Sensen Wu: Data curation, Formal analysis, Methodology, Software. Guangtao Xia: Conceptualization, Funding acquisition, Project administration, Validation, Writing – review & editing.

Funding

This work was supported by the Natural Science Foundation of Shandong Province (ZR2021MH265) and Jinan Clinical Medical Science and Technology Innovation Plan (202019051).

Supplementary materials

Supplementary material associated with this article can be found in the online version at doi:10.1016/j.aohep.2023.101183.

References

[1] Manns MP, Lohse AW, Vergani D. Autoimmune hepatitis—update 2015. J Hepatol 2015;62(1 Suppl):S100–11. https://doi.org/10.1016/j.jhep.2015.03.005.
[2] Arase Y, Matsumoto K, Anzai K, Tsuruya K, Sugiyama S, Yoshihara S, et al. Clinicopathological features of autoimmune hepatitis with IgG4-positive plasma cell infiltration. Dig Dis 2021;39(3):225–33. https://doi.org/10.1159/000510562.
[3] Kunitomo K, Ohkuchi A, Matsumoto S, Wada M, Himeno R, Sakamoto T. Gradual improvement of hyperammonemic hepatic encephalopathy after the extirpation of a large uterine leiomyoma in a woman with constipation and liver cirrhosis resulting from autoimmune hepatitis. J Obstet Gynaecol Res 2016;42(3):353–7. https://doi.org/10.1111/jog.12900.
[4] Sucher E, Sucher R. Autoimmune hepatitis-immunologically triggered liver pathogenesis-diagnostic and therapeutic strategies. 2019;2019:9437043. https://doi.org/10.1155/2019/9437043.
[5] Lu TX, Rothenberg ME. MicroRNA. J Allergy Clin Immunol 2018;141(4):1202–7. https://doi.org/10.1016/j.jaci.2017.08.034.
[6] Essandoh K, Li Y, Huo J, Fan GC. MiRNA-mediated macrophage polarization and its potential role in the regulation of inflammatory response. Shock 2016;46(2):122–31. https://doi.org/10.1097/shk.0000000000000604.
[7] Xia G, Wu S, Wang X, Fu M. Inhibition of microRNA-155 attenuates concanavalin—a-induced autoimmune hepatitis by regulating Treg/Th17 cell differentiation. Can J Physiol Pharmacol 2018;96(12):1293–300. https://doi.org/10.1139/cjpp-2018-0467.
[8] Ingwersen J, Menge T, Wingerath B, Kaya D, Graf J, Prozorovski T, et al. Natalizumab restores aberrant miRNA expression profile in multiple sclerosis and reveals a critical role for miR-20b. Ann Clin Transl Neurol 2015;2(1):43–55. https://doi.org/10.1002/acn3.152.
[9] Zhao N, Zou H, Qin J, Fan C, Liu Y, Wang S, et al. MicroRNA-326 contributes to autoimmune thyroiditis by targeting the Ets-1 protein. Endocrine 2018;59(1):120–9. https://doi.org/10.1007/s12020-017-1465-4.
[10] Zhang J, Liu Y, Shi G. The circRNA-miRNA-mRNA regulatory network in systemic lupus erythematosus. Clin Rheumatol 2021;40(1):331–9. https://doi.org/10.1007/s10067-020-05212-2.
[11] Coutinho DF, Monte-Mór BC, Vianna DT, Rouxinol ST, Batalha AB, Bueno AP, et al. TET2 expression level and 5-hydroxymethylcytosine are decreased in refractory cytopenia of childhood. Leuk Res 2015;39(10):1103–8. https://doi.org/10.1016/j.leukres.2015.07.005.
[12] Ichiyama K, Chen T, Wang X, Yan X, Kim BS, Tanaka S, et al. The methylcytosine dioxygenase Tet2 promotes DNA demethylation and activation of cytokine gene expression in T cells. Immunity 2015;42(4):613–26. https://doi.org/10.1016/j.immuni.2015.03.005.
[13] Oh YJ, Shin DY, Hwang SM, Kim SM, Im K, Park HS, et al. Mutation of ten-eleven translocation-2 is associated with increased risk of autoimmune disease in patients with myelodysplastic syndrome. Korean J Intern Med 2020;35(2):457–64. https://doi.org/10.3904/kjim.2018.247.
[14] Tan L, Fu L. TET2 regulates 5-hydroxymethylcytosine signature and CD4(+) T-cell balance in allergic rhinitis. 2022;14(2):254-72. https://doi.org/10.4168/aair.2022.14.2.254.
[15] Ji C, Nagaoka K, Zou J, Casulli S, Lu S, Cao KY, et al. Chronic ethanol-mediated hepatocyte apoptosis links to decreased TET1 and 5-hydroxymethylcytosine formation. FASEB J. 2019;33(2):1824–35. https://doi.org/10.1096/fj.201800736R.
[16] Tanaka S, Ise W, Inoue T, Ito A, Ono C, Shima Y, et al. Tet2 and Tet3 in B cells are required to repress CD86 and prevent autoimmunity. 2020;21(8):950-61. https://doi.org/10.1038/s41590-020-0700-y.
[17] Li J, Li L, Sun X, Deng T, Huang G, Li X, et al. Role of Tet2 in regulating adaptive and innate immunity. Front Cell Dev Biol 2021;9:665897. https://doi.org/10.3389/fcell.2021.665897.
[18] Jang Y, Lee AY, Jeong SH, Park KH, Paik MK, Cho NJ, et al. Chlorpyrifos induces NLRP3 inflammasome and pyroptosis/apoptosis via mitochondrial oxidative stress in human keratinocyte HaCaT cells. Toxicology 2015;338:37–46. https://doi.org/10.1016/j.tox.2015.09.006.
[19] Luan J, Zhang X, Wang S, Li Y, Fan J, Chen W, et al. NOD-like receptor protein 3 inflammasome-dependent IL-1β accelerated cona-induced hepatitis. Front Immunol 2018;9:758. https://doi.org/10.3389/fimmu.2018.00758.
[20] Wang Z, Zhang S. NLRP3 inflammasome and inflammatory diseases. 2020;2020:4063562. https://doi.org/10.1155/2020/4063562.
[21] Lei L, Sun J, Han J, Jiang X, Wang Z, Chen L. Interleukin-17 induces pyroptosis in osteoblasts through the NLRP3 inflammasome pathway in vitro. Int Immunopharmacol 2021;96:107781. https://doi.org/10.1016/j.intimp.2021.107781.
[22] Takeuchi Y, Ohara D, Watanabe H, Sakaguchi N, Sakaguchi S, Kondoh G, et al. Dispensable roles of Gsdmd and Ripk3 in sustaining IL-1β production and chronic inflammation in Th17-mediated autoimmune arthritis. Sci Rep 2021;11(1):18679. https://doi.org/10.1038/s41598-021-98145-y.
[23] Li LL, Dai B, Sun YH, Zhang TT. The activation of IL-17 signaling pathway promotes pyroptosis in pneumonia-induced sepsis. Ann Transl Med 2020;8(11):674. https://doi.org/10.21037/atm-19-1739.
[24] Ma L, Jiang M, Zhao X, Sun J, Pan Q, Chu S. Cigarette and IL-17A synergistically induce bronchial epithelial-mesenchymal transition via activating IL-17R/NF-κB signaling. 2020;20(1):26. https://doi.org/10.1186/s12890-020-1057-6.
[25] Hao J, Sun W, Xu H. Pathogenesis of Concanavalin A induced autoimmune hepatitis in mice. Int Immunopharmacol 2022;102:108411. https://doi.org/10.1016/j.intimp.2021.108411.
[26] Zhang F, Xiao L, Yang Y, Zhou M, Zhao Y, Xie Z, et al. Human menstrual blood-derived stem cells alleviate autoimmune hepatitis via JNK/MAPK signaling pathway in vivo and in vitro. Front Med 2023. https://doi.org/10.1007/s11684-022-0953-y.
[27] Jiang H, Fang Y, Wang Y, Li T, Lin H, Lin J, et al. FGF4 improves hepatocytes ferroptosis in autoimmune hepatitis mice via activation of CISD3. Int Immunopharmacol 2023;116:109762. https://doi.org/10.1016/j.intimp.2023.109762.
[28] Elshal M, Hazem SH. Escin suppresses immune cell infiltration and selectively modulates Nrf2/HO-1, TNF-α/JNK, and IL-22/STAT3 signaling pathways in concanavalin A-induced autoimmune hepatitis in mice. Inflammopharmacology 2022. https://doi.org/10.1007/s10787-022-01058-z.
[29] Zhu J, Chen H, Cui J, Zhang X, Liu G. Oroxylin A inhibited autoimmune hepatitis-induced liver injury and shifted Treg/Th17 balance to Treg differentiation. Exp Anim 2023. https://doi.org/10.1538/expanim.22-0171.
[30] Loubaki L, Hadj-Salem I, Fakhfakh R, Jacques E, Plante S, Boisvert M, et al. Co-culture of human bronchial fibroblasts and CD4+ T cells increases Th17 cytokine signature. PLoS One 2013;8(12):e81983. https://doi.org/10.1371/journal.pone.0081983.
[31] Hou L, Jie Z, Desai M, Liang Y, Soong L, Wang T, et al. Early IL-17 production by intrahepatic T cells is important for adaptive immune responses in viral hepatitis. J Immunol 2013;190(2):621–9. https://doi.org/10.4049/jimmunol.1201970.
[32] Gao G, Wang Z, Lu L, Duan C, Wang X, Yang H. Morphological analysis of mitochondria for evaluating the toxicity of α-synuclein in transgenic mice and isolated preparations by atomic force microscopy. Biomed Pharmacother 2017;96:1380–8.
[33] Komori A. Recent updates on the management of autoimmune hepatitis. Clin Mol Hepatol 2021;27(1):58–69. https://doi.org/10.3350/cmh.2020.0189.
[34] Vuerich M, Wang N, Kalbasi A, Graham JJ, Longhi MS. Dysfunctional immune regulation in autoimmune hepatitis: from pathogenesis to novel therapies. Front Immunol 2021;12:746436. https://doi.org/10.3389/fimmu.2021.746436.
[35] Jadideslam G, Ansarin K, Sakhinia E, Babaloo Z, Abhari A, Alipour S, et al. Expression levels of miR-21, miR-146b and miR-326 as potential biomarkers in Behcet's disease. 2019;13(16):1339-48. https://doi.org/10.2217/bmm-2019-0098.
[36] Honardoost MA, Kiani-Esfahani A, Ghaedi K, Etemadifar M, Salehi M. miR-326 and miR-26a, two potential markers for diagnosis of relapse and remission phases in patient with relapsing-remitting multiple sclerosis. Gene 2014;544(2):128–33. https://doi.org/10.1016/j.gene.2014.04.069.
[37] Sukma Dewi I, Hollander Z, Lam KK, McManus JW, Tebbutt SJ, Ng RT, et al. Association of serum MiR-142-3p and MiR-101-3p levels with acute cellular rejection after heart transplantation. PLoS One 2017;12(1):e0170842. https://doi.org/10.1371/journal.pone.0170842.
[38] Sebastiani G, Grieco FA, Spagnuolo I, Galleri L, Cataldo D, Dotta F. Increased expression of microRNA miR-326 in type 1 diabetic patients with ongoing islet autoimmunity. Diabetes Metab Res Rev 2011;27(8):862–6. https://doi.org/10.1002/dmrr.1262.
[39] Jin L, Fang X, Dai C, Xiang N, Tao J, Sun X, et al. The potential role of Ets-1 and miR-326 in CD19(+)B cells in the pathogenesis of patients with systemic lupus erythematosus. Clin Rheumatol 2019;38(4):1031–8. https://doi.org/10.1007/s10067-018-4371-0.

[40] Ahmadi M, Yousefi M. Disturbed Th17/Treg balance, cytokines, and miRNAs in peripheral blood of patients with Behcet's disease. 2019;234(4):3985-94. https://doi.org/10.1002/jcp.27207.
[41] Wu CT, Huang Y, Pei ZY, Xi X, Zhu GF. MicroRNA-326 aggravates acute lung injury in septic shock by mediating the NF-κB signaling pathway. Int J Biochem Cell Biol 2018;101:1–11. https://doi.org/10.1016/j.biocel.2018.04.019.
[42] Rui J, Deng S, Perdigoto AL. Tet2 controls the responses of β cells to inflammation in autoimmune diabetes. 2021;12(1):5074. https://doi.org/10.1038/s41467-021-25367-z.
[43] Stefan-Lifshitz M, Karakose E, Cui L, Ettela A, Yi Z, Zhang W, et al. Epigenetic modulation of β cells by interferon-α via PNPT1/mir-26a/TET2 triggers autoimmune diabetes. JCI insight 2019;4(5). https://doi.org/10.1172/jci.insight.126663.
[44] Zhaolin Z, Jiaojiao C, Peng W, Yami L, Tingting Z, Jun T, et al. OxLDL induces vascular endothelial cell pyroptosis through miR-125a-5p/TET2 pathway. 2019;234(5):7475-91. https://doi.org/10.1002/jcp.27509.
[45] Carrillo-Jimenez A, Deniz Ö, Niklison-Chirou MV, Ruiz R, Bezerra-Salomão K, Stratoulias V, et al. TET2 regulates the neuroinflammatory response in microglia. Cell Rep 2019;29(3):697–713 e8. https://doi.org/10.1016/j.celrep.2019.09.013.
[46] Ma Q, Dasgupta C, Shen G, Li Y, Zhang L. MicroRNA-210 downregulates TET2 and contributes to inflammatory response in neonatal hypoxic-ischemic brain injury. J Neuroinflammation 2021;18(1):6. https://doi.org/10.1186/s12974-020-02068-w.